Fatigue of Aircraft Structures
Vol. 1 (2011) 28-41
10.2478/v10164-010-0035-5

THE ANALYSIS OF FATIGUE CRACK PROPAGATION IN THE ELEMENTS OF ALUMINUM ALLOY D16CZATW WITH A NOTCH IN THE FORMOF A CYLINDRICAL HOLE

Volodymyr Hutsaylyuk
Janusz Mierzyński
Dariusz Zasada

Military University of Technology
Warsaw, Poland

Abstract

In this work, the fatigue life of specimens made from the aluminum alloy D16CzATW has been determined. To this aim, flat specimens with notches in the form of cylindrical holes made by drilling and reaming have been investigated. The research was carried out under the conditions of constant-amplitude bending at the stress ratio of R = -1. The results obtained were compared with the fatigue life of specimens with calibrated holes and specimens without notches. Fatigue life was determined for specimens plated on both sides and those without this protecting layer. Very large differences in fatigue resistance were observed. These differences can be explained by the negative effect of the brittle protecting layer on the fatigue crack initiation process. A complex fracture mechanism was observed, in which micro-mechanisms of brittle and ductile fracture were appearing at different stages of fatigue crack propagation.

1. INTRODUCTION

Aluminum alloys are commonly used in the aircraft industry for skin of aircraft fuselages and wings. Flight safety requires knowledge of the fatigue properties of those alloys, especially in the presence of a notch. The processes that occur within the area of a notch significantly affect durability and operational safety of the whole structures. This work presents an analysis of processes occurring during initiation and early propagation of fatigue cracks in the elements of aluminum alloy D16CzATW with the central cylindrical hole. This stage is important from the point of view of evaluating maximum allowable crack lengths as well as forecasting fatigue life for short fatigue cracks [1].

The aluminum alloy D16CzATW is an equivalent of a widely used 2024-T3 alloy and is produced and used in aircraft structures in Russia and Central-East European countries. A characteristic feature of these alloys is a combination of good fatigue and anti-corrosive properties.

The analysis of the problem with reference to D16CzATW alloy is very difficult because only some publications regarding the fatigue fracture of this alloy are available in the international journals. These are mostly Russian publications, which are not easily accessible and of local character. Those which deserve particular attention concern fatigue behaviour of D16 alloy and its different modifications [2-6], with a special emphasis on investigating the failure mechanisms of structural elements for different variants of cyclical load.

In Polish literature, publications [7-10] deserve detailed attention. These works give fatigue crack propagation rates in D16 alloy for six various research programmes, which encompass 12 variants of loads. The constant-amplitude tests at different asymmetry coefficients R and maximum stress levels constituted the main part of experimental research. Fracture surfaces were subjected to detailed analysis at macro and micro levels. A detailed comparison of the University's own research results with literature-based data concerning 2024 alloy was conducted. Special attention was paid to a negative effect of a protecting plated layer on fatigue life of aluminum alloys as well as to a considerable decrease in strength alongside with increase in thickness of the specimens.

There are many publications regarding fatigue life and description of fatigue crack development in the 2024 alloy, which is equivalent to D16 alloy.

Comparative research of fatigue life and fatigue crack development in the 2024 and D16 alloys are described in work [11]. Flat specimens with a central notch were subject to steady–amplitude bending. Research of crack propagation was supported by the microfractographic analysis with application of a transmitting electronic microscope (TEM). No significant differences in the mechanism of initiation or kinetics of fatigue cracks propagation for both alloys were observed. Fatigue life was predicted based on the probability model, which provided results consistent with experimental ones.

The results of fatigue tests conducted on specimens made from the 2024 aluminum alloy with a calibrated hole are presented in [12]. Research was conducted at a positive coefficient of asymmetry. Several series of specimens made from sheets of a thickness of 1.26-mm, with various degrees of calibration in the range of 0.3 % to 6.9 %, were tested. It was noted that fatigue life improved alongside with an increase of the calibration degree. The reason for this improvement was investigated using numerical simulation of the calibration process [13]. The results obtained indicate that the hole calibration introduces additional circumferential compressive stresses, which decrease the effect of stress concentration from the hole, and therefore, make it difficult to initiate and develop fatigue cracks.

In the publications [14-15] attention was mainly paid to investigation of the possibility of reconstructing fatigue fracture rates, in elements made from 2024-T3 alloys, based on the macro- and microfractographic analysis of the fracture surfaces. Flat specimens with a central notch were subjected to load equal to the service load in the lower skin of aircraft wings. Research results concerning the kinetics of fatigue crack development were presented in the form of classical graphs of crack rates in relation to crack length, the number of recurrences of load blocks, stress intensity factor and the ratio of the number of cycles to the number of cycles to failure. The results were correlated with fracture rates determined based on the fatigue striations, which were obtained during microfractographic tests. There were observed limitations for the possibility of reconstructing the service load spectrum based on the analysis of fracture surfaces in failed structural components in the case of complex loads.

2. MATERIAL, SPECIMENS, RESEARCH METHODOLOGY

2.1. Material

Research was conducted on specimens made from Russian D16CzATW aluminum alloy. The additional marking of the alloy is deciphered as follows: Cz – alloy of high purity, A –plated, T – natural aging, W – applied in aviation. The material was received in the form of 2.75-mm-thick sheets that were plated on both sides. According to the manufacturer's certificate, it should possess the following mechanical properties: Rm = 442–463 MPa, Re = 316–328 MPa, E = 69.35 GPa and $A5$ = 18.8–21.2 %. Chemical composition of the material is presented in Table 1. Random tests have confirmed the manufacturer's data.

Table 1. Amount of elements in the chemical composition of D16CzATW

	Cu	Mg	Mn	Si	Fe	Ti	Zn	Cr
Manufacturer Data	%							
	4,4	1,4	0,63	0,11	0,18	0,07	0,01	0,01

The microstructure of the material delivered was characteristic of the cold-deformed materials. The microstructure in two mutually perpendicular planes is shown in Figure 1. The thickness of the visible protective layer is approximately 70 μm, as shown in Fig. 1b.

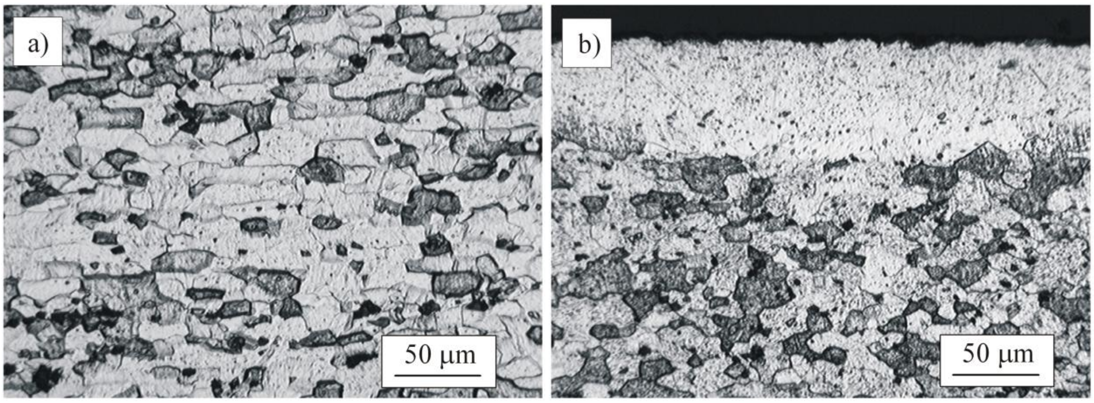

Fig. 1. Microstructure of D16CzATW alloy in the plane of rolling direction (a) and in the plane perpendicular to rolling direction (b)

2.2. Research Methodology

Fatigue life tests were conducted with the use of flat specimens, the shape of which is shown in Fig. 2. The central hole with the diameter of 4 mm was obtained by drilling to the size of ∅ 3,8 mm and then reamed to the size of ∅ 4 mm. The specimens were cut in the direction of material rolling during manufacturing.

Fatigue life tests were conducted under conditions of flat bending on the testing fixture illustrated in Fig. 3. Loading was realized under the coefficient of asymmetry cycle $R = -1$ and load frequency of 25 Hz. The testing fixture consists of the following elements: the base (1), with a support for securing a specimen (2), and the motor (3). The load acting on a specimen is applied by a spring, not shown in this picture, which is pulled by the lever shoulder (4). The change of the load for consecutive specimens was realized by change of the connection of the lever shoulder with the turning disk (5). The stress levels were controlled by the measuring system (6) using a template sample with a glued extensometer. Statistical evaluation was performed as per the ASTM E739-91 standards.

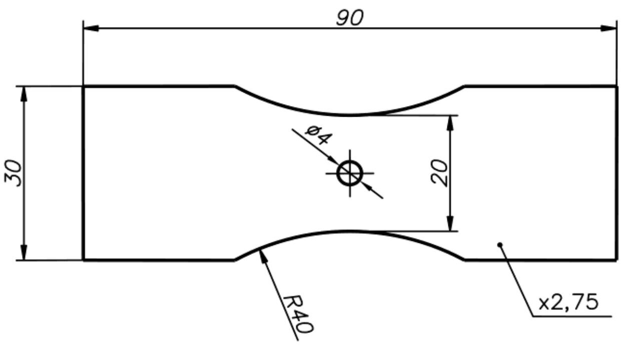

Fig. 2. Specimen for fatigue tests

For a given specimen geometry, additional tests were performed for the purpose of fatigue resistance evaluation after removing the plated layer. These tests were performed in order to verify the information about the adverse effect of the plated layer on fatigue resistance of the elements under the conditions of stretching.

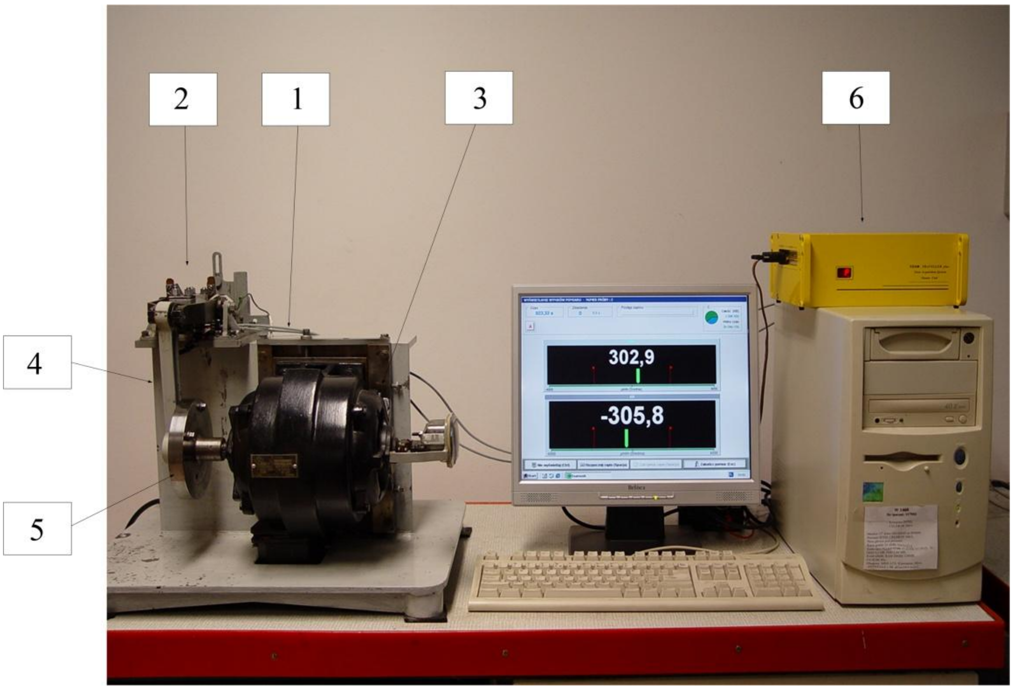

Fig. 3. Test fixture for the research of fatigue resistance and the registration of crack propagation

The geometry of the specimen allowed observing the crack development with aid of acetate-cellulose replicas. Each time the machine was stopped, two replicas were placed in the area of the forecasted break. Before the replicas were placed, the specimens had been preliminarily statically loaded in order to open a fatigue crack. The observation was conducted in the whole range of specimens' strength, so as to obtain at least 20 crack length measurements. The replicas were researched with the use of an optical microscope.

The analysis of the mechanism of crack propagation into the depth of the material was realized during fractographic research of fracture surfaces with the use of the PHILIPS XL-30 and SEM Quanta 3D-FEG scanning electron microscopes.

3. TEST RESULTS AND DISCUSSION

3.1. Fatigue resistance of specimens with a geometric notch in the form of a cylindrical hole

Research on fatigue resistance of specimens plated on both sides with a notch in the form of a drilled and reamed hole and the diameter of 4 mm was conducted for 10 specimens and 5 levels of bending stress within the range of 102 MPa to 178 MPa. This level of load was corresponding to the interval from 30% to 53% of the plasticity border R_e for the tested material. The weakening of the specimen by the hole and stress concentration was not taken into account in the calculations of the amplitude of bending stress. Detailed results of testing are shown in Fig. 4.

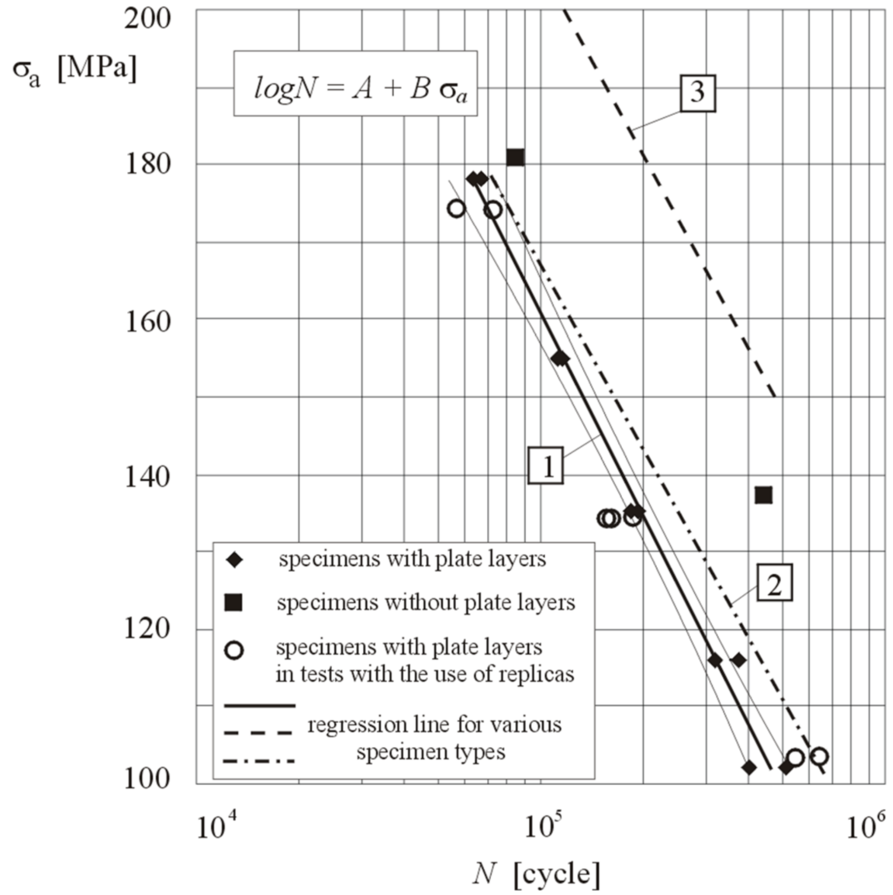

Fig. 4. Fatigue resistance of D16CzATW alloy for different variations of specimen preparation

Equation of a simple regression (2) was determined in accordance with the ASTM E739-91 standards; its parameters are shown in Table 2.

$$log N = A + B \cdot \sigma_a \tag{2}$$

where: N- fatigue life of a specimen, σ_a – bending stress amplitude,

A more detailed analysis of research results allows noting a good repeatability of fatigue life tests results at respective load levels. Almost all results are located within the band drafted for the accepted 95% confidence level, which is restricted by limiting hyperbolas plotted in the graph. Such repeatability is a result of the homogenous structure and the presence of a strong initiator in the form of a hole, which unified the initiation phase and the beginning of fatigue crack propagation for all specimens in a given series. The interval of confidence parameters $\hat{A}$ and $\hat{B}$ for the results of the base research series is estimated in following manner: $\hat{A}$ (6,86126-7,28286) and $\hat{B}$ (-0,01461-0,01143).

The results of fatigue life tests for the specimen for which we measured crack propagation by the method of replicas, were plotted against the background of the base series results. The conditions of these tests differ from the base tests in delay of load and multiple removal of specimen from fixtures for static loading and putting the replicas on. The result of this is a greater spread of fatigue life of specimens in relation to the regression line defined based on the results of the base series of specimens (line 1). It can be assumed that testing of fatigue crack propagation with use of replicas provides us with greater spread, but does not influence basic processes of fracture mechanisms, which are observed in specimens under continuous load. The results obtained confirm insignificant effect of the testing methodology with use of replicas on fatigue life of D16CzATW alloy.

Interesting results were obtained during testing of fatigue life of specimens with a hole and without a plated layer. The increase in fatigue resistance was noted in correlation to plated specimens. The value of the increase constitutes around 27% at σ_a = 180 MPa to 140% at σ_a = 135 MPa. These results should be interpreted with a certain caution due to a small number of specimens being tested. They cannot, however, be neglected during the fatigue resistance analysis of D16CzATW alloy.

Table 2. Parameters of equations that describe specimens' fatigue resistance of specimens with a different geometry of a notch

Line Number	Type of a specimen	Parameters of Equation(2)	
		A	B
1	Specimens with drilled and reamed holes	7,07206	-0,01302
2	Specimens with drilled and calibrated holes	7,1342	-0,01279
3	Specimens without a notch	7,41966	-0,01154

Against the background of the results of specimens with drilled and reamed holes, simple regressions obtained during testing of specimens plated on both sides with a hole drilled and calibrated (line 2), and specimens without a notch (line 3) were presented. It was noted, that the process of calibration increases fatigue resistance of specimens. However, this increase is not great and equals around 15 % under the greatest stress and around 35% under the smallest stress. More detailed information about specimen testing results with drilled and calibrated holes is provided in [16]. Fatigue resistance of specimens plated on both sides without a notch (line 3) was 3 to 4 times higher, depending on the level of load, in relation to specimens with drilled and reamed holes.

3.2. Initiation and propagation of fatigue cracks

Fatigue testing of the specimens (Fig. 2) revealed a significant decrease in resistance as compared to both the specimens with calibrated holes and those without notches. This was due to the fact that the weakening caused by the hole and the stress concentration were not taken into account in calculations of critical section load. Besides, the crack propagation processes differ for all these cases. The basic process differences at the initiation and fatigue crack propagation stage at macroscopic level are described below.

The fracture of a specimen with a notch in the form of a hole occurred as a result of the development of four quarter-elliptical cracks, which were always initiated on the top and bottom surface of the specimen at the hole. Such a localization of the source of crack initiation is associated with a significant stress concentration due to a notch. The cracks were developing in pairs in parallel planes. Eventually, they joined with a clearly visible leap, which caused fracturing. The regions of final fracture are visible from one side on the profile of the specimen. The almost smooth surface of some fracture fragments testifies to successive development of each quarter-elliptical crack from the one source. This is clearly visible in Fig 5, which shows the fracture of the specimen with a dye applied three times after a given number of cycles.

Fig. 5. Fracture of plated specimen with cylindrical hole after bending
σ_a = 103 MPa (N_f = 507 400 cycles)

In Fig. 6, the fracture of a specimen with a cylindrical hole after removing the plated layer is shown. About 100 μm of material from each side was removed by hand polishing. The development of dominant fatigue cracks at a micro-level is similar to the development of those on plated specimens. The difference in fatigue strength must have resulted from a difference in the moment of initiation of fatigue cracks and lack of additional micro-cracks, which are initiated from the surface of the specimen in its middle part, as in the case of specimens without a notch (Fig. 8).

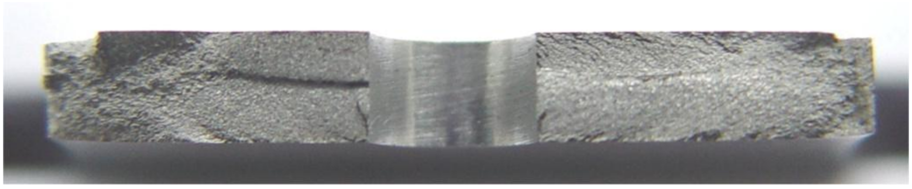

Fig. 6. Fracture of a specimen with a cylindrical hole without a layer of plate after bending
σ_a = 181 MPa (N_f = 84 500 cycles)

Such crack propagation completely differs from specimens with a calibrated cylindrical hole (Fig. 7). In this case, total fatigue resistance of a specimen depends on cracks which initiated from outside edges of a specimen or random sources, but not from the hole. A more detailed description of this complex fatigue fracture process is provided in [16].

Fig. 7. Fracture of a specimen with cylindrical calibrated hole after bending
(σ_a = 133 MPa, N_f = 213 200 cycles)

A quite different crack propagation process occurred in the specimens without a notch, whose fatigue resistance strongly depended on independent development of many micro-cracks, which propagated from both plated surfaces and edges of a specimen (Fig. 8).

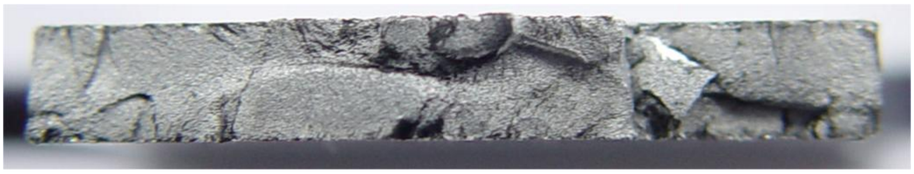

Fig. 8. Fracture of a specimen without a notch after bending
σ_a = 164 MPa (N_f = 415 400 cycles)

3.3. Micro-fractographic research

A full analysis of fracture mechanisms of specimens with a cylindrical hole was performed on the basis of fractographical results obtained with the use of a scanning electronic microscope. Two specimens, with a plated layer and without, were investigated. Fig. 9 shows a magnified specimen fracture, which was tested at the bending stress amplitude σ_a = 102 MPa. In the picture, the areas of further fractographic analysis are shown. The places in the vicinity of the crack source were selected: the regions of stable propagation of fatigue crack; the region passing to the region of final-fracture and the region of final-fracture for one of dominant quarter elliptical cracks. Details are shown in Figure 10. For the same orientation, the microfractografic photograph in Fig. 9 should be turned 90° to the right. The source of cracks is easy to identify as located in the plated layer next to the hole (upper right corner in Fig. 10a). The plated layer clearly differs from the native material, characterised by instant propagation of a crack. Under this layer, a crack is propagating radially in all directions from the initiator. Instant propagation of a crack in the plated layer is confirmed in Fig. 10b, where the source of the crack is presented at higher magnification. The characteristic signs of brittle trans-crystal fracture are visible.

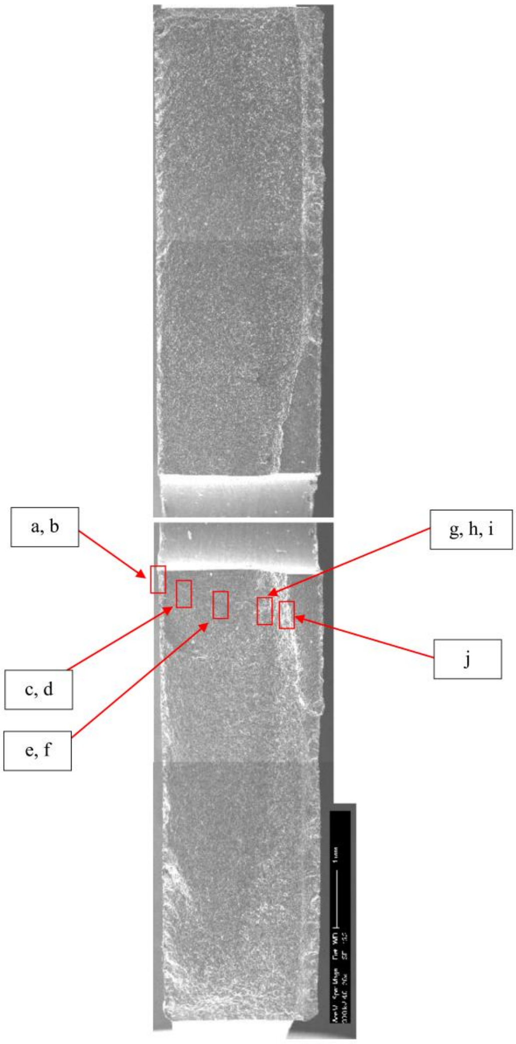

Fig. 9. Fracture of specimen with a plate layer and cylindrical hole after bending σ_a = 102 MPa (N_f = 509 300 cycle)

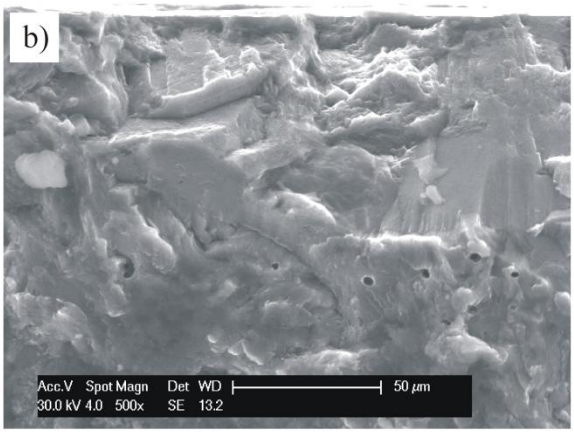
b)
Acc.V Spot Magn Det WD 50 μm
30.0 kV 4.0 500x SE 13.2

90°

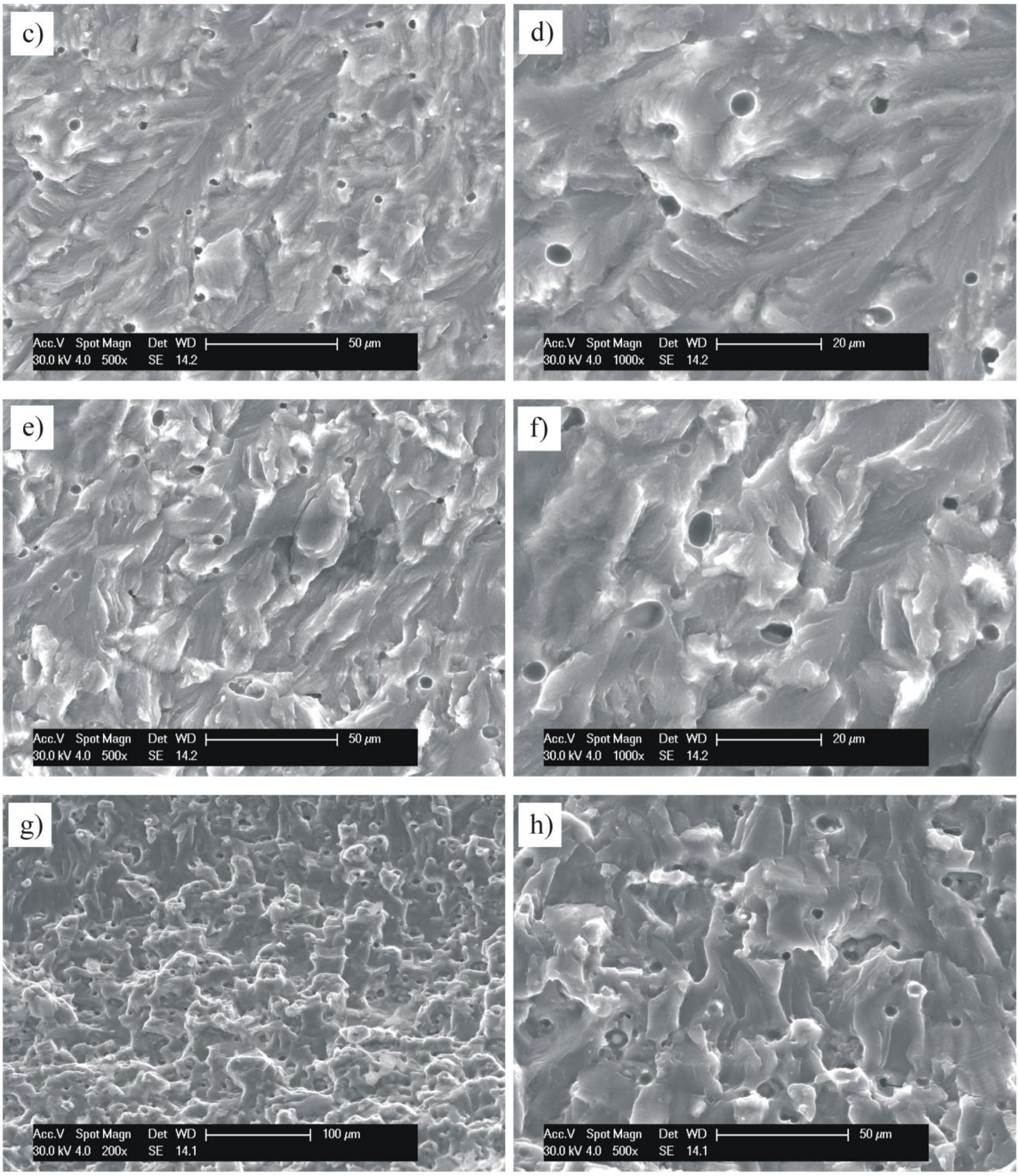
c)
Acc.V Spot Magn Det WD 50 μm
30.0 kV 4.0 500x SE 14.2
d)
Acc.V Spot Magn Det WD 20 μm
30.0 kV 4.0 1000x SE 14.2
e)
Acc.V Spot Magn Det WD 50 μm
30.0 kV 4.0 500x SE 14.2
f)
Acc.V Spot Magn Det WD 20 μm
30.0 kV 4.0 1000x SE 14.2
g)
Acc.V Spot Magn Det WD 100 μm
30.0 kV 4.0 200x SE 14.1
h)
Acc.V Spot Magn Det WD 50 μm
30.0 kV 4.0 500x SE 14.1

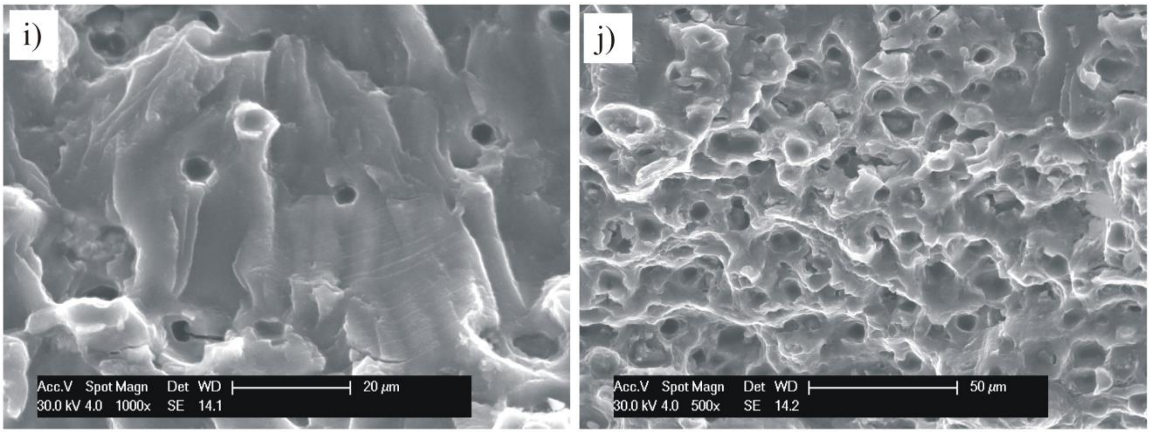

Fig. 10. Pictures of specimen fracture with a plate layer, drilled and reamed hole after bending σ_a = 102 MPa (explanation in the text)

After leaving the plated layer a crack is developing steadily at an increasing rate. In Fig. 10 c, d, a fracture picture of this stage of crack development is shown at 600 μm from the source and at 1400 μm from the source of crack in Fig. 10 e,f. The analysis of the pictures shown revealed presence of insignificant plastic deformations on the borders of the marked micro volumes. Those micro volumes are covered by numerous micro slips, which create characteristic patterns of a pine tree (10 d) or fanning (10 f). In the second picture, relatively large and almost smooth volumes of the size comparable to the material grains are shown. Those volumes, resembling the facets of a cleavage fracture, are covered with multidirectional fatigue striations Fig. 11, which can be seen only by using a SEM Quanta 3D-FEG microscope.

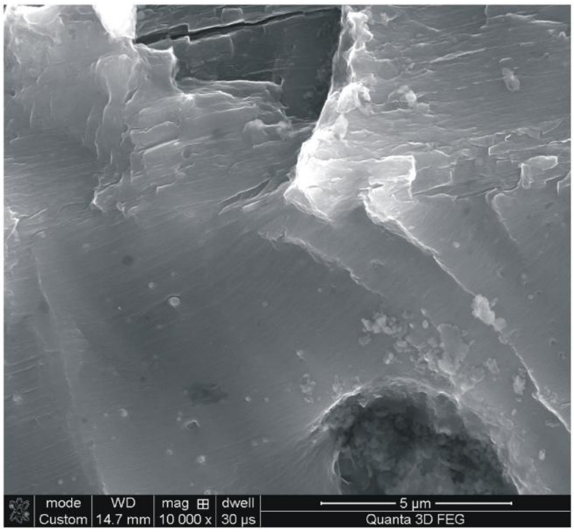

Fig. 11. Magnified fracture of a specimen under bending amplitude stress σ_a = 102 MPa

Figures 10 g-i are showing the passing from a region of stable propagation to a narrow band of the final fracture zone created at the contact point of two quarter-elliptical dominating cracks. This passing is clearly marked. The following photographs are made at increasing magnification and show the increasing contribution of plastic deformation to the process of fracture. The borders of the marked micro volumes are more elongated, secondary cracks and systems of fatigue striations with greater intervals are present (Fig. 10i). The last picture in Figure 10 is typical of the zone of final fracture in the form of the homogenous plate-like structure. In this small volume formed on the border of two quarter-elliptical macro-cracks, fracturing with strong plastic deformation prevailed.

Fig. 12 shows a photograph of fracturing in the selected half of the specimen fracture, tested at bending stress amplitude of $\sigma_a = 155$ MPa, which is significantly larger than previous. It was attempted to establish differences in mechanisms of fracture of specimens depending on the stress level. In Fig. 12, two quarter-elliptical cracks, which come out from the plated layer in the area of the hole, are clearly marked. In the case of this specimen, additional cracks, which initiated from the plated layer beyond the region of a notch (hole), for example from the outside left upper corner of the specimen, came to our attention. The possible appearance of such additional sources of cracks in the plated layer needs to be considered in calculation models during prediction of fatigue life of structures elements made from plated alloy D16CzATW. In the photograph, places for further analysis at greater magnification are marked. Microfractografic analysis has proved that fracture on the micro-scale is qualitatively very similar to this presented in the prior photograph. The only change is intensity of appearance, which is explained by higher values of bending stress amplitude. Therefore, the photographs below show the selected places which are characteristic for the corresponding regions of fatigue crack propagation.

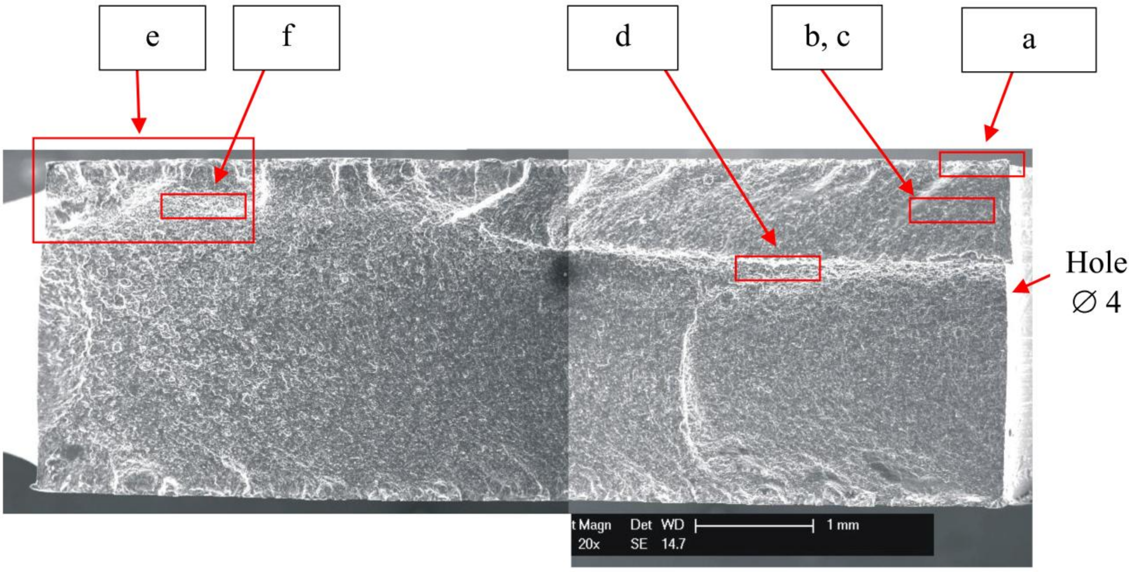

Fig. 12. Left side of a pattered fractured specimen under bending stress amplitude σ_a = 155 MPa (N_f = 112 600 cycles)

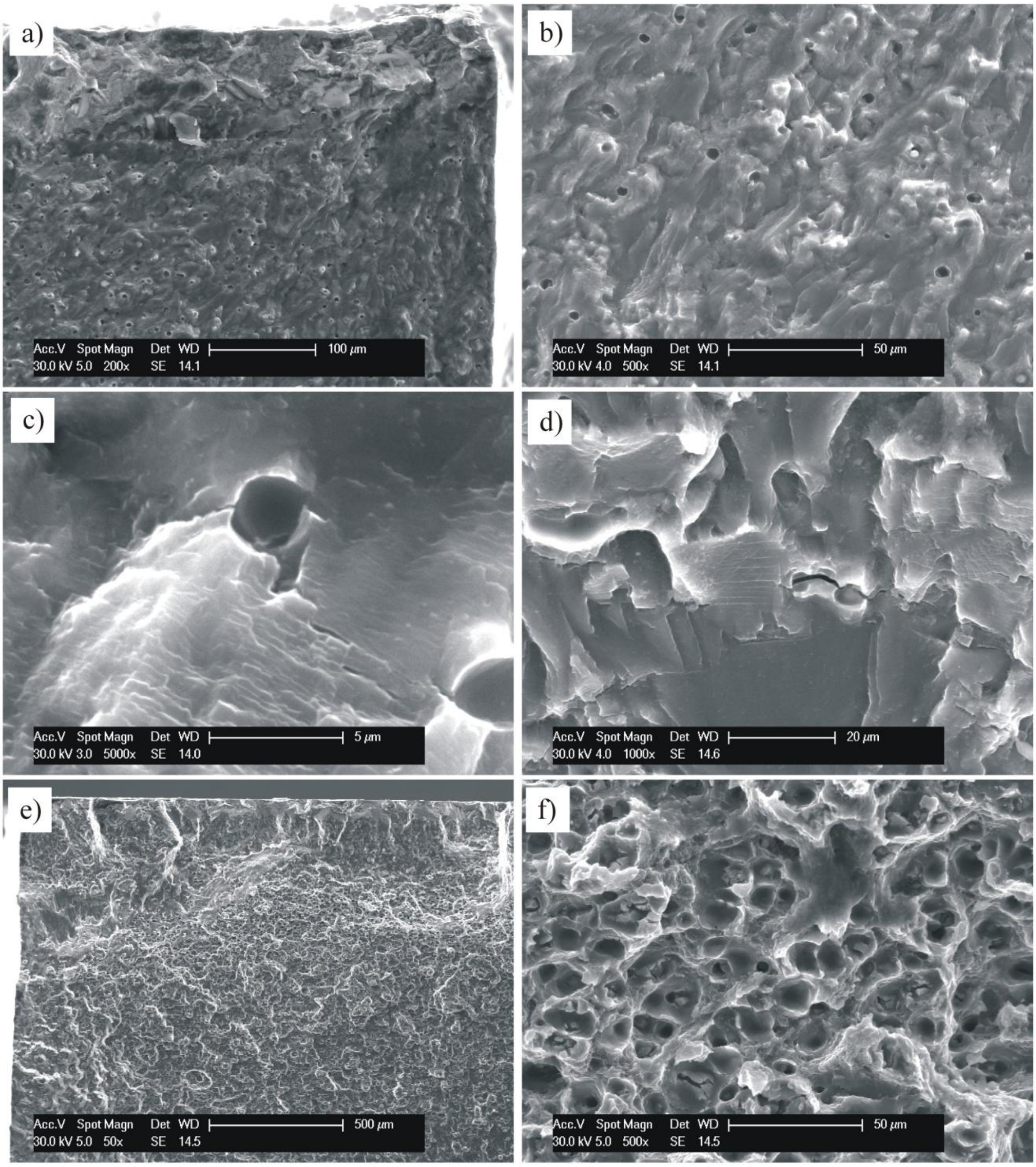

Fig. 13. Photograph of fractures of plated specimen with drilled and reamed hole after bending under amplitude of σ_a = 155 MPa

4. SUMMARY

The research was realized under the conditions of constant-amplitude bending at stress ratio asymmetry cycle of R = -1. Fatigue resistance graphs were obtained for specimens with drilled and reamed holes, and also for specimens plated on both sides and those without this protecting layer. The results obtained were compared to the results obtained for the specimens without a notch and those with a calibrated hole.

The good repeatability of the tests results due to high monogamy of microstructure of the D16CzATW alloy was noted. Fatigue resistance of a specimen with a drilled and reamed hole was 3-4 times lower than that of a specimen without a notch. It has been established that the calibration beneficially affects fatigue resistance of a specimen. In the case of specimens subjected to calibration at the degree of k = 3,25 %, fatigue life increased in the range between 15 % and 35 % depending on the level of bending stress amplitude as compared to specimens with holes that were not strengthened. Also, an unfavourable effect of plated layers on a fatigue failure process was observed. After removal of the plated layer, fatigue resistance of specimens with drilled and reamed holes increased from 27% at bending stress amplitude σ_a = 180 MPa to 140 % at σ_a = 135 MPa in relation to plated specimens. This layer is the source of a great number of surface microcracks, which accelerate fracturing.

This behavior was investigated in the process of analysis of micro fracture mechanisms. Microfractographic analysis of fracture surfaces revealed in the native material numerous signs of brittle and quasi-brittle fracturing with few plastic deformations. An increase in cracking depth was accompanied by the intensification of plastic deformation. The formation of multi-directionally oriented systems of fatigue striations and a great number of secondary cracks were also observed.

REFERENCES:

[1] Miller, K.J. (1982). Short crack problem. *Fatigue of Engineering Materials and Structures*. 5(1982), 223-232. DOI: 10.1111/j.1460-2695.1982.tb01250.x

[2] Kornev, V., Karpov, E. & Demeshkin, A. (2010). Damage accumulation in the pre-fracture zone under low-cyclic loading of specimens with the edge crack. Procedia Engineering, 2 (1), 465-474.

[3] Radchenko, O.I., Cabezas Morales, A.J. & Zvyagin, S.V. (1998). The diagram of bifurcation points for process of the fatigue of aluminium D16-alloy. *Metallofizika i Noveishie Tekhnologii*. 20 (5), 72-79.

[4] Klevtsov, G.V., Botvina, L.R. & Klevtsova, N.A. (1996). Plastic zones formation under different types of loading conditions. *ISIJ International*. 36 (2), 215-221.

[5] Lebedev, A.A., Chausov, N.G., Boginich, I.O. & Nedoseka, S.A. (1996). Complex evaluation of damage to material in plastic deformation process. *Problemy Prochnosti*. (5), 23-30.

[6] Klevtsov, G.V., Botvina, L.R., Gorbatenko, N.A. & Klevtsov, R.G. (1995). The influence of cycle asymmetry and loading scheme on fractographical and structural features of alloy type D16 fatigue fractures. Izvestiya Akademii Nauk SSSR. *Metally*, (2), 145-152.

[7] Skorupa, M., Skorupa, A., Machniewicz, T. & Gruszczyński, P. (2002). Wzrost pęknięć zmęczeniowych w lotniczym stopie aluminium. XIX Sympozjum Zmęczenie i Mechanika Pękania, Bydgoszcz - Pieczyska, 2002 (pp. 361-368).

[8] Skorupa, M., Skorupa, A., Machniewicz, T. & Gruszczyński, P. (2003). Trendy eksperymentalne we wzroście pęknięć zmęczeniowych w blasze z lotniczego stopu aluminium D16, *Przegląd Mechaniczny*. 11(2003), 21-27.

[9] Skorupa, M., Skorupa, A. & Machniewicz, T. (2004). Efekty interakcji obciążeń we wzroście pęknięć zmęczeniowych w stopie aluminium D16Cz. XX Sympozjum Zmęczenie i Mechanika Pękania, Bydgoszcz - Pieczyska, 2004 (pp. 387-394).

[10] Schijve, J. Skorupa, M., Skorupa, A., Machniewicz, T. & Gruszczyński, P. (2004). Fatigue crack growth in the aluminium alloy D16 under constant and variable amplitude loading. *International Journal of Fatigue*. 26(2004), 1-15.

[11] Śnieżek, L. (2005). Badania powstawania i rozwoju pęknięć zmęczeniowych w stopach aluminium stosowanych na pokrycia statków latających z uwzględnieniem wpływu działania karbu. Sprawozdanie z realizacji pracy badawczej własnej nr 827, WAT, Warszawa.

[12] Mroziński, S. & Lipski, A. (2009). Eksperymentalna analiza kalibracji otworów nitowych. XXIV Sympozjum Podstaw Konstrukcji Maszyn, 2009 (pp. 359-364).

[13] Lipski, A. & Mroziński, S. (2009). Numeryczna symulacja procesu kalibrowania otworu pod nit. XXIV Sympozjum Podstaw Konstrukcji Maszyn, Białystok -Białowieża, 2009, (pp. 310-315).

[14] Kocańda, D., Kocańda, S. & Torzewski, J. Variable amplitude load interaction in fatigue crack growth for 2024T3 aluminium alloy. Proc. 16th European Conf. of Fracture ECF-16, Greece, 2006, Ed. E.E. Gdoutos, pp. 177-178 (abstract).

[15] Kocańda, D. &Torzewski, J. (2006). Capability of load-time history reconstruction and fatigue growth rate estimation for 2024T3 aluminium alloy on the basis of fractographic analysis. Proc. Intern Conf. of Mechanical Fatigue of Metals, Ternopil, Ukraine 2006, (pp. 42-48).

[16] Mierzyński, J. & Hutsaylyuk, V. (2010). The micromechanism of fatigue cracking of the D16 aluminium alloy elements with a calibrated hole subject to bending, XV International Colloquium Mechanical Fatigue of Metals, Opole, 2010.